Multilayer Asymmetric Aperture-Coupled Broadside Microstrip Lines and Their Quasi-Static and Dynamic Analyses

Subbarao Kunasani and Cam Nguyen, *Senior Member, IEEE*

***Abstract*— This paper describes new multilayer aperture-coupled broadside microstrip lines suitable for miniaturized microwave and millimeter-wave integrated circuits. Spectral-domain method is used for detailed investigations of these structures, and both quasi-static and dynamic results are presented to illustrate the need of a full-wave analysis for accurate circuit designs at high frequencies. The new transmission lines possess many desirable features, such as flexibility in circuit design and ability to optimize various transmission lines' characteristics, as well as miniaturization by using thin dielectric layers. Besides having the inherent properties of large ratios for the mode characteristic impedances and effective dielectric constants found in broadside-coupled structures, we also found that the studied coupled transmission lines can have equal mode effective dielectric constants for certain values of the structural parameters.**

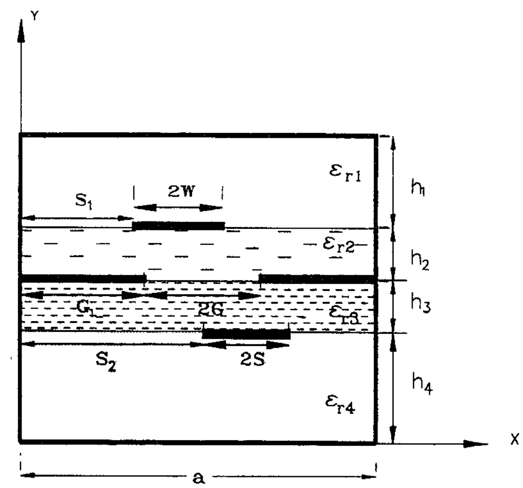

Fig. 1. Cross section of the new multilayer asymmetric aperture-coupled broadside microstrip lines.

I. Introduction

In the past two decades, we have witnessed a rapid advancement of microwave and millimeter-wave hybrid (MIC) and monolithic (MMIC) integrated circuits for both civilian and military applications. Toward this end, many planar transmission lines have been proposed and used. Recent efforts have concentrated on reducing the sizes of current MMIC's through the use of thin-film microstrip lines fabricated on thin dielectric substrates over a GaAs semi-insulating substrate [1]–[4]. The thin-film microstrip lines have narrow line widths because of the use of very thin dielectric layers, thus making high-density circuit integration feasible. However, these structures are single transmission lines and, therefore, are not applicable for MMIC's using parallel coupled lines, such as filters and couplers. Multilayer thin-film coupled transmission lines can be employed to solve this problem while achieving very compact, high-density circuit integration.

In this paper we propose and study new multilayer aperture-coupled microstrip lines (Fig. 1) suitable for miniaturized MIC's and MMIC's. They consist of two dielectric layers (e.g., silicon oxynitride), isolated by a common ground plane, over a grounded dielectric substrate (e.g., GaAs). The bottom ground plane is used to increase the mechanical strength as well as to facilitate the heat dissipation and packaging needed for practical applications. The two coupled strips have unequal widths and are asymmetrically located on two different layers. These strips are coupled to each other through an arbitrarily located coupling aperture on the common ground plane. Arbitrary locations for the strips and coupling slot are attractive as they allow the transmission lines' parameters, such as couplings, characteristic impedances and velocities, to be optimized for a particular application. Through the use of thin dielectric layers, narrow line-widths can also be obtained, resulting in compact circuits. The proposed structures can have significantly less distortion via appropriate selection of the dielectric layers, as discovered for multilayer microstrip lines [5]. A similar structure, referred to as "double-sided substrate microstrip lines" consisting of two dielectric substrates and two microstrip lines coupled through a rectangular slot, was analyzed [6], [7]. However, the reported structure is not suitable for MMIC's, and to some extent MIC's, since the substrates are assumed to be identical and suspended in the air. It is basically a stripline-type transmission line and clearly not applicable to MMIC's. In addition, its upper and lower strips are of equal width and symmetrically located on top of each other, thereby limiting the transmission line's flexibility in circuit design and the ability to optimize the transmission line's characteristics.

Manuscript received August 28, 1995; revised August 29, 1995. This work was supported in part by Innovasia, Inc.

The authors are with the Department of Electrical Engineering, Texas A&M University, College Station, TX 77843-3128 USA.

IEEE Log Number 9415562.

0018–9480/95$04.00

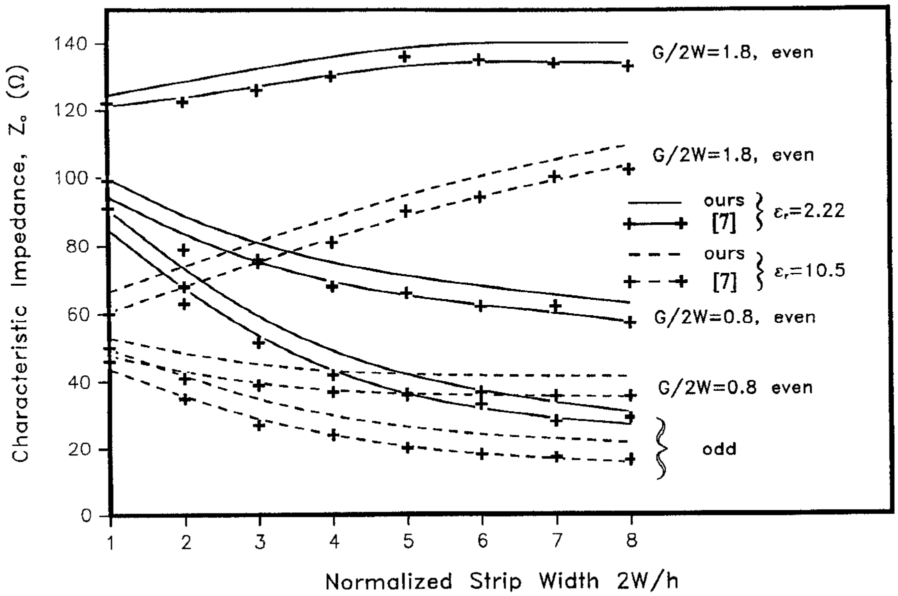

Fig. 2. Dynamic characteristic impedances and effective dielectric constants for double-sided substrate microstrip lines versus 2 W/h. a = 125 mils, $h_1 = h_4 = 2$ mm, $h_2 = h_3 = h = 0.254$ mm, $\varepsilon_{r1} = \varepsilon_{r4} = 1, \varepsilon_{r2} = \varepsilon_{r3} = \varepsilon_r, f = 10$ GHz.

II. Analysis

Fig. 1 shows the cross section of the multilayer asymmetric aperture-coupled microstrip lines. The enclosure, ground planes, and strips are assumed to be perfect conductors. Additionally, the dielectric substrates and the metallization are assumed to be lossless and infinitesimally thin, respectively. This structure supports two quasi–TEM modes designated as c- and π-modes. Both the quasi-static and dynamic analyses are carried out based on the spectral-domain approach (SDA) [8], [9] and are performed for the shielded structure, as shown in Fig. 1. Results can be applied to the open version by setting appropriate values to the structural parameters. The SDA is well documented, and hence, only brief formulations are given here.

A. Quasi-Static Analysis

By using the quasi-static SDA, which utilizes Galerkin's method described in [8], we obtain the following set of coupled linear algebraic equations

$$\sum_{m=1}^{M} P_{11}^{im} c_m + \sum_{k=1}^{K} P_{12}^{ik} d_k + \sum_{n=1}^{N} P_{13}^{in} f_n = Q_i, \qquad i = 1, 2, \ldots, M.$$

$$\sum_{m=1}^{M} P_{21}^{jm} c_m + \sum_{k=1}^{K} P_{22}^{jk} d_k + \sum_{n=1}^{N} P_{23}^{jn} f_n = 0, \qquad j = 1, 2, \ldots, K.$$

$$\sum_{m=1}^{M} P_{31}^{lm} c_m + \sum_{k=1}^{K} P_{32}^{lk} d_k + \sum_{n=1}^{N} P_{33}^{ln} f_n = 0, \qquad l = 1, 2, \ldots, N.$$

where

$$P_{11}^{im} = \sum_{m=1}^{M} \tilde{\rho}_{SUi} \tilde{G}_{11} \tilde{\rho}_{SLm}$$

$$P_{12}^{ik} = \sum_{k=1}^{K} \tilde{\rho}_{SUi} \tilde{G}_{12} \tilde{\rho}_{gk}$$

$$P_{13}^{in} = \sum_{n=1}^{N} \tilde{\rho}_{SUi} \tilde{G}_{13} \tilde{\rho}_{SLn}$$

$$P_{21}^{jm} = \sum_{m=1}^{M} \tilde{\rho}_{gj} \tilde{G}_{21} \tilde{\rho}_{SUm}$$

$$P_{22}^{jk} = \sum_{k=1}^{K} \tilde{\rho}_{gj} \tilde{G}_{22} \tilde{\rho}_{gk}$$

$$P_{23}^{jn} = \sum_{n=1}^{N} \tilde{\rho}_{gj} \tilde{G}_{23} \tilde{\rho}_{SLn}$$

$$P_{31}^{lm} = \sum_{m=1}^{M} \tilde{\rho}_{SLl} \tilde{G}_{31} \tilde{\rho}_{SUm}$$

$$P_{32}^{lk} = \sum_{k=1}^{K} \tilde{\rho}_{SLl} \tilde{G}_{32} \tilde{\rho}_{gk}$$

$$P_{33}^{1n} = \sum_{n=1}^{N} \tilde{\rho}_{SLl} \tilde{G}_{33} \tilde{\rho}_{SUn}$$

$$Q_i = \int_{S1}^{S1+2w} \rho_{SUi} dx + \int_{S2}^{S2+2s} \rho_{SLi} dx.$$

$\tilde{G}$'s represent the spectral domain Green's functions; c_m, d_k and f_n are unknown coefficients associated with known basis functions ρ_{SU}, ρ_{SL} and ρ_g that describe the charge distributions on the upper, lower strips and the common ground plane, respectively. The tilde ($\sim$) indicates the Fourier-transformed quantity.

Constants c_m, d_k, and f_n can now be determined from the above equations, from which the charge distributions on the strips can be obtained. We then follow the procedure described in [10] to determine the mode characteristic impedances and

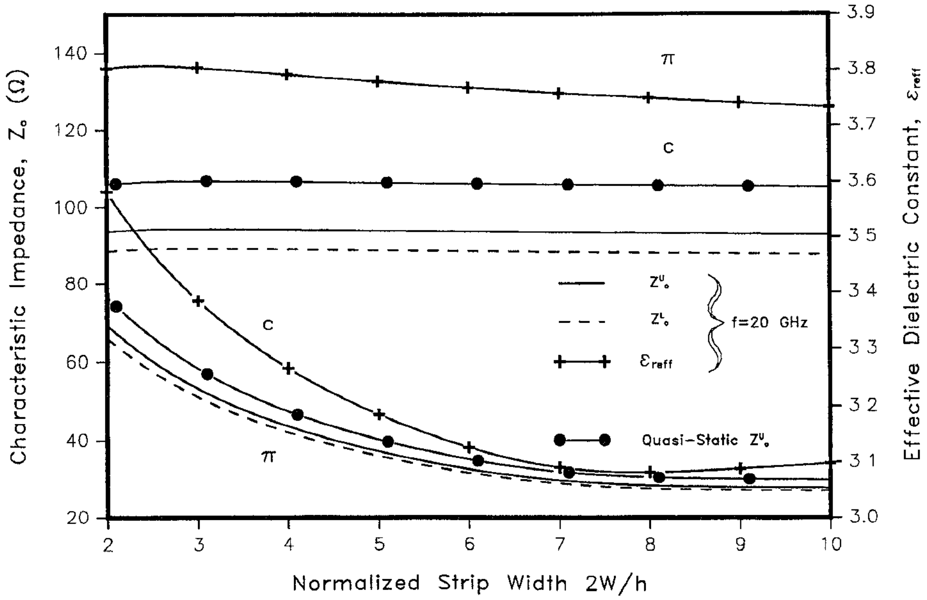

Fig. 3. Characteristic impedances and effective dielectric constants for an asymmetrical aperture-coupled structure versus 2 W/h. $a = 125$ mils, $h_1 = 100$ mils, $h_2 = h_3 = h = 5$ μm, $h_4 = 25$ mils, $S_1 = 30$ mils, $G_1 = 35$ mils, $S_2 = 70$ mils, $2G = 8$ mils, $2S = 16$ mils, $\varepsilon_{r1} = 1$, $\varepsilon_{r2} = \varepsilon_{r3} = 3.3$ (polyimide), $\varepsilon_{r4} = 12.9$ (GaAs).

effective dielectric constants. We first determine the per-unit-length capacitances corresponding to equal and opposite potential excitations on the two strips. We then evaluate the c- and π-mode capacitances per unit length and the corresponding mode characteristic impedances and effective dielectric constants.

B. Dynamic Analysis

Applying the SDA [9] produces the following coupled linear algebraic equations

$$\sum_{m=1}^{M} P_{11}^{im}(\beta)c_m + \sum_{k=1}^{K} P_{12}^{ik}(\beta)d_k + \sum_{n=1}^{N} P_{13}^{in}(\beta)f_n = 0, \quad i = 1,2,\ldots,M.$$

$$\sum_{m=1}^{M} P_{21}^{jm}(\beta)c_m + \sum_{k=1}^{K} P_{22}^{jk}(\beta)d_k + \sum_{n=1}^{N} P_{23}^{jn}(\beta)f_n = 0, \quad j = 1,2,\ldots,K.$$

$$\sum_{m=1}^{M} P_{31}^{lm}(\beta)c_m + \sum_{k=1}^{K} P_{32}^{lk}(\beta)d_k + \sum_{n=1}^{N} P_{33}^{ln}(\beta)f_n = 0, \quad l = 1,2,\ldots,N.$$

where

$$P_{11}^{im} = \sum_{r=1}^{R} \tilde{J}_{uxi}(\alpha_r)\tilde{G}_{11}(\alpha_r,\beta)\tilde{J}_{uxm}(\alpha_r)$$

$$P_{12}^{ik} = \sum_{r=1}^{R} \tilde{J}_{uxi}(\alpha_r)\tilde{G}_{12}(\alpha_r,\beta)\tilde{J}_{uzk}(\alpha_r)$$

$$P_{13}^{in} = \sum_{r=1}^{R} \tilde{J}_{uzi}(\alpha_r)\tilde{G}_{13}(\alpha_r,\beta)\tilde{J}_{uzn}(\alpha_r)$$

$$P_{21}^{jm} = \sum_{r=1}^{R} \tilde{J}_{uxi}(\alpha_r)\tilde{G}_{21}(\alpha_r,\beta)\tilde{J}_{uzm}(\alpha_r)$$

$$P_{22}^{jk} = \sum_{r=1}^{R} \tilde{J}_{uxi}(\alpha_r)\tilde{G}_{22}(\alpha_r,\beta)\tilde{J}_{lxk}(\alpha_r)$$

$$P_{23}^{jn} = \sum_{r=1}^{R} \tilde{J}_{lxi}(\alpha_r)\tilde{G}_{23}(\alpha_r,\beta)\tilde{J}_{uzn}(\alpha_r)$$

$$P_{31}^{lm} = \sum_{r=1}^{R} \tilde{J}_{lxi}(\alpha_r)\tilde{G}_{31}(\alpha_r,\beta)\tilde{J}_{lxm}(\alpha_r)$$

$$P_{32}^{lk} = \sum_{r=1}^{R} \tilde{J}_{lxi}(\alpha_r)\tilde{G}_{32}(\alpha_r,\beta)\tilde{J}_{lzk}(\alpha_r)$$

$$P_{33}^{1n} = \sum_{r=1}^{R} \tilde{J}_{lzi}(\alpha_r)\tilde{G}_{33}(\alpha_r,\beta)\tilde{J}_{lzn}(\alpha_r)$$

J_{ux}, J_{uz} and J_{lx}, J_{lz} are the x, z, current distributions of the upper and lower strips, respectively; c's, d's, and f's are unknown coefficients associated with these current components; G's are the Green's functions in the spectral domain; β is the propagation constant; and α_r is the Fourier-transform variable. We now set the determinant of the coefficient matrix of the above equations to zero to obtain the propagation constants of both the c- and π-modes, from which the effective dielectric constants can be calculated. The c- and π-mode characteristic impedances of the upper and lower strips are calculated using the formula $Z_0 = \frac{2P_{\text{avg}}}{I_0^2}$, where P_{avg} represents the average power transmitted across the transmission line's cross section, and I_0 is the strip current.

III. Numerical Results

To verify the analysis, we computed the c- and π-mode quasi-static and dynamic characteristic impedances and ef-

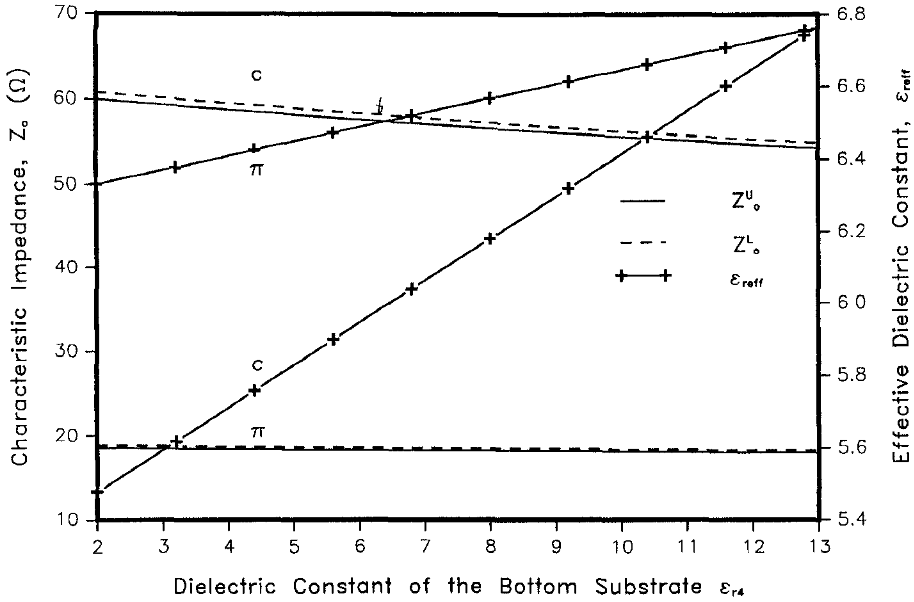

Fig. 4. Dynamic characteristic impedances and effective dielectric constants for an asymmetrical aperture-coupled structure versus ε_{r4}. All parameters are the same as in Fig. 3, except $h_2 = h_3 = h = 2$ μm, $2W = 6$ mils, $2S = 4$ mils $\varepsilon_{r2} = \varepsilon_{r3} = 7$ (Si_3N_4), $f = 20$ GHz.

fective dielectric constants for a "double-sided substrate microstriplines" structure consisting of two identical substrates suspended in the air and compared with the results in [7]. Fig. 2 shows our results for the dynamic characteristic impedances and those in [7, Fig. 9] versus the normalized strip width. The discrepancy is less than 2.5%, which can be attributed to the fact that [7] employed both the current and electric field distributions whereas our results are based only on the current distributions. Similar agreement is also obtained for all of the other cases. It should be noted here that our c- and π-mode parameters are identical to those of the even- and odd-modes, respectively, used in [7], since the considered structure is symmetrical.

Fig. 3 shows variations of the characteristic impedances and effective dielectric constants for an asymmetric aperture-coupled structure as a function of the upper strip's normalized width at a frequency of 20 GHz. It is seen that as the upper-strip width is increased, the π-mode characteristic impedances and c-mode effective dielectric constant reduce, whereas the c-mode characteristic impedances and π-mode effective dielectric constant remain virtually the same. The data suggest that large ratios for the mode characteristic impedances and effective dielectric constants can be obtained by increasing the upper- or lower-strip width. This is an inherent property of broadside-coupled structures [10]. Quasi-static results for the c- and π-mode characteristic impedances of the upper strip are also included and, as can be seen, the difference between these and the dynamic values at 20 GHz is around 11%, indicating the need of a full-wave analysis for accurate circuits designs.

Results of the characteristic impedances and effective dielectric constants for an asymmetric structure at 20 GHz as the relative dielectric constant of the grounded bottom substrate changes are shown in Fig. 4. It is noticed that the c- and π-mode characteristic impedances are almost the same for both strips in this case. This phenomenon is expected as the two layers between the strips are identical and relatively very thin as compared to the grounded bottom substrate, resulting in a strong confinement of the fields within these layers. It is seen that the bottom substrate's dielectric constant has no significant effect on the mode characteristic impedances. However, while the π-mode effective dielectric constant only varies less than 7%, that for the c-mode changes substantially. Furthermore, it is interesting to observe that the effective dielectric constants for the c- and π-modes are equal when the dielectric constant of the bottom substrate is 12.8. This result can be exploited to design directional couplers with maximum isolation.

Fig. 5 shows effects of the coupling aperture's normalized width on the characteristic impedances and effective dielectric constants for an asymmetric structure. It is seen that increasing this width slightly increases the c-mode characteristic impedances, while keeping the π-mode counterparts almost constant. It is also clear that both the c- and π-mode effective dielectric constants decrease as the width is increased. Again, we notice that the c- and π-mode effective dielectric constants coincide at certain values of the aperture width.

Values of the mode characteristic impedances and effective dielectric constants for an asymmetric structure are plotted as a function of the ratio of the dielectric constants of the substrates above and below the common ground plane in Fig. 6. As can be seen, all the characteristic impedances decrease while the effective dielectric constants increase as the ratio is increased.

A remark that needs to be made at this point is that all of the presented data are applicable to open versions of the considered transmission lines, as the upper layer was assumed to be air and the enclosure width as well as the upper layer thickness were relatively large.

IV. Conclusion

We have proposed and studied new multilayer asymmetric aperture-coupled microstrip lines for possible uses in MIC's

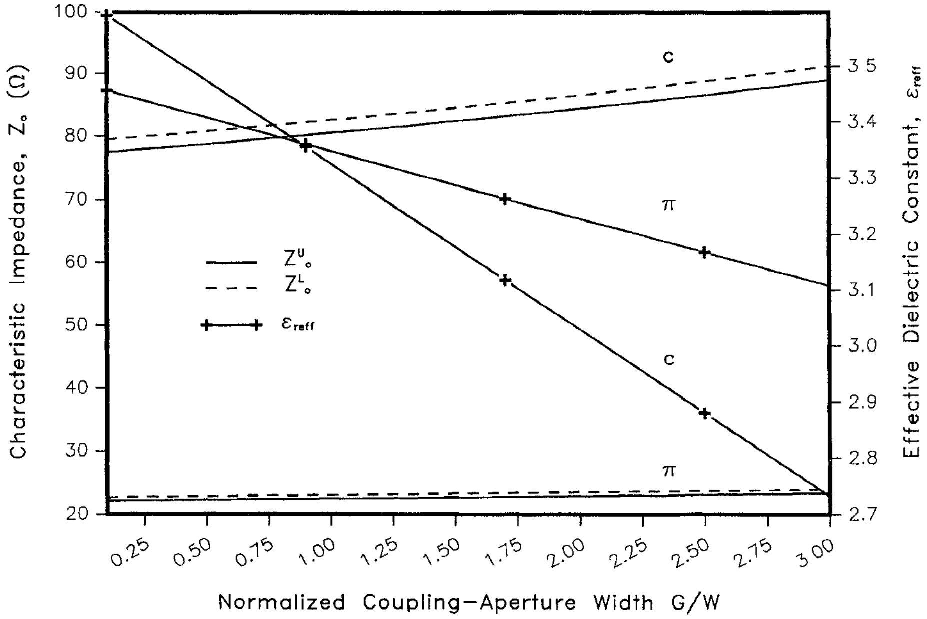

Fig. 5. Dynamic characteristic impedances and effective dielectric constants for an asymmetrical aperture-coupled structure versus G/W. All dimensions are the same as in Fig. 4 except $\varepsilon_{r4} = 12.9$.

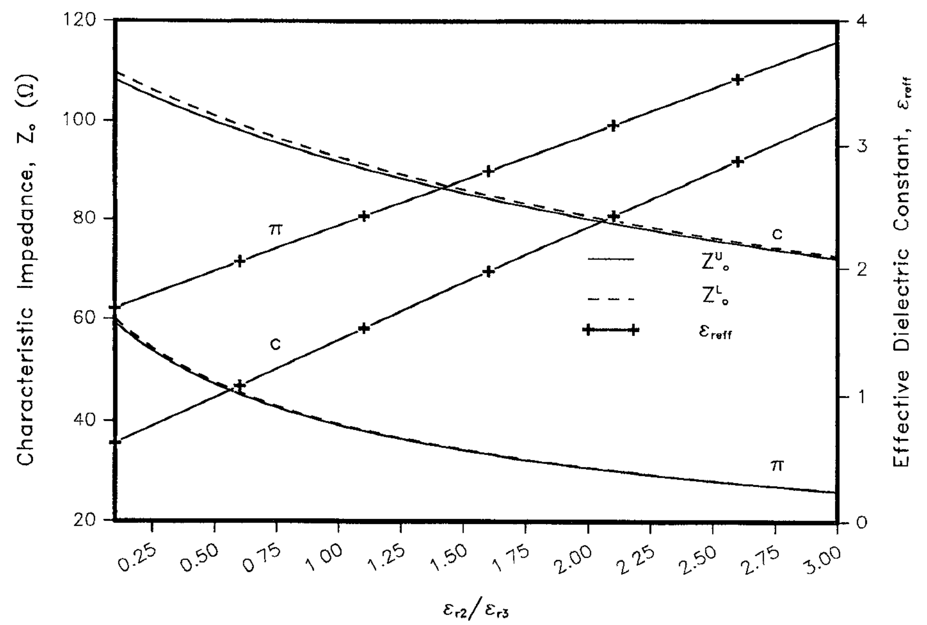

Fig. 6. Dynamic characteristic impedances and effective dielectric constants for an asymmetrical aperture-coupled structure versus $\varepsilon_{r2}/\varepsilon_{r3}$. All the dimensions are the same as in Fig. 4 except $h_2 = h_3 = h = 4$ μm, $\varepsilon_{r4} = 12.9$.

and MMIC's. These transmission lines are completely general, in which the strips and coupling aperture can be arbitrarily located. They, besides having all of the inherent characteristics of broadside-coupled structures, can have equal mode effective dielectric with appropriate structural parameters' values. Miniaturized MIC's and MMIC's are also feasible by using thin dielectric layers. Numerical results also indicate that a full-wave analysis should be used for accurate circuit designs. The proposed transmission lines and their analyses should be useful for possible applications in MIC's and MMIC's.

Acknowledgment

The authors wish to thank the anonymous reviewers for their useful comments and suggestions.

References

[1] S. Banba *et al.*, "Multilayer MMIC branchline hybrid thin dielectric layers," *IEEE Microwave Guided Wave Lett.*, vol. 1, pp. 346–347, Nov. 1991.

[2] T. Hiraoka *et al.*, "Very small wide-band MMIC magic T's using microstrip lines on a thin dielectric film," *IEEE Trans. Microwave Theory Tech.*, vol. 37, pp. 1569–1575, Oct. 1989.

[3] H. Ogawa *et al.*, "MMIC transmission lines for multi-layered MMIC's," in *1991 IEEE MTT-S Int. Microwave Symp. Dig.*, pp. 1067–1070.

[4] T. Tokumitsu *et al.*, "Multilayer MMIC using a 3 μm X 3-layer dielectric layers," in *1990 IEEE MTT-S Int. Microwave Symp. Dig.*, pp. 831–834.

[5] J. P. K. Gilb and C. A. Balanis, "Asymmetric multi-conductor low-coupling structures for high-speed, high-density digital integrated circuits," *IEEE Trans. Microwave Theory Tech.*, vol. 39, pp. 2100–2106, Dec. 1991.

[6] T. Tanaka *et al.*, "Slot-coupled directional couplers between double-sided substrate microstrip lines and their applications," *IEEE Trans. Microwave Theory Tech.*, vol. 36, pp. 1752–1757, Dec. 1988.

[7] M. F. Wong *et al.*, "Analysis and design of slot-coupled directional couplers between double-sided substrate microstrip lines," *IEEE Trans. Microwave Theory Tech.*, vol. 39, pp. 2123–2129, Dec. 1991.

[8] T. Itoh and A. S. Hebert, "A generalized spectral domain analysis for coupled suspended microstriplines with tuning septum's," *IEEE Trans. Microwave Theory Tech.*, vol. MTT-26, pp. 820–826, Oct. 1978.

[9] T. Itoh and R. Mittra, "A technique for computing dispersion characteristics of shielded microstriplines," *IEEE Trans. Microwave Theory Tech.*, vol. MTT-22, pp. 896–898, Oct. 1974.

[10] C. Nguyen, "Broadside-coupled coplanar waveguides and their end-coupled band-pass filter applications," *IEEE Trans. Microwave Theory Tech.*, vol. 40, pp. 2181–2189, Dec. 1992.

Subbarao Kunasani received the B.Tech. degree in electronics and communication engineering from Jawaharlal Nehru Technological University, India, and the M.Tech. degree in microwave engineering from the Indian Institute of Technology, India. He is currently pursuing the Ph.D. degree in electrical engineering at Texas A&M University.

He worked at the Indian Institute of Technology and Bharat Electronics Ltd. in India in 1991.

Mr. Kunasani received the National Merit Scholarship, State Merit Scholarship, and Ministry of Human Resources awards in 1982, 1984, and 1989, respectively.

Cam Nguyen (S'82–M'83–SM'91) received the B.S. degree in mathematics from the National University of Saigon, Vietnam, and the B.S., M.S., and Ph.D. degrees in electrical engineering from California Polytechnic University, Pomona, California State University, Northridge, and the University of Central Florida, respectively.

From 1979 to 1982, he was employed by ITT Gilfillan, Van Nuys, CA, where he designed and developed various microwave components for ground- and ship-based radars, including power dividers and combiners, filters, frequency doublers and triplers, phase shifters, switches, and power amplifiers. In 1982, he joined Hughes Aircraft Co. in Torrance, CA, as a member of the technical staff and worked on many millimeter-wave components, from 26.5–150 GHz, including mixers, switches, and filters. From 1983 to 1986, he was with TRW, Redondo Beach, CA, where he was responsible for the design and development of advanced millimeter-wave integrated-circuit components, from 26.5–170 GHz, including finline and crossbar mixers, subharmonic mixers, multiplexers, filters, oscillators, frequency multipliers, phase shifters, amplifiers, and switches. He also developed various computer programs for the analysis and design of microwave and millimeter-wave integrated circuits. From 1986 to 1987, he was with Aerojet ElectroSystems Co., Azusa, CA, where he was responsible for the design and development of extremely low-noise, space-qualified mixers from 60–110 GHz for radiometry applications. In 1987, he joined the monolithic group of Martin Marietta Co., Orlando, FL. There he was responsible for the design and development of millimeter-wave monolithic circuits. He was also involved with the development of microstrip and CPW discontinuity models and nonlinear models for MESFET's and HEMT's. In 1989 he returned to the Communication Laboratory of TRW, Redondo Beach, CA, as a Senior Staff Engineer, where he was responsible for the development of advanced microwave and millimeter-wave components and subsystems, such as high dynamic range MMIC mixers and multichannel switched filters, etc. In 1991 he joined the faculty of the Department of Electrical Engineering of the Texas A&M University. His current research interests encompass both the areas of electromagnetics and microwave electronics with concentrations in the microwave and millimeter-wave circuits, devices, planar transmission lines, receivers, and transmitters. He has published more than 75 papers and two book chapters.